

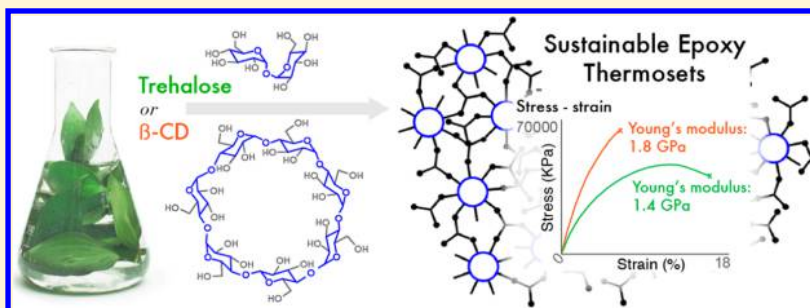
Epoxy Resin Thermosets Derived from Trehalose and β -Cyclodextrin

Quanxuan Zhang,[†] Monika Molenda,[‡] and Theresa M. Reineke*,[†]

[†]Department of Chemistry and Center for Sustainable Polymers, University of Minnesota, 207 Pleasant Street SE, Minneapolis, Minnesota 55455, United States

[‡]Oakland University, Rochester, Michigan 48309, United States

Supporting Information



ABSTRACT: Epoxy resins are ubiquitous in high-performance composite applications because of their excellent mechanical strength, thermal and chemical resistance, strong adhesion, and low shrinkage after curing. Bio-based epoxy resins derived from natural products such as carbohydrates offer tremendous potential for creating new polymeric materials. Sugars and their derivatives often offer great biodegradability and functionality such as the presence of multiple hydroxyl groups that impart highly cross-linked polymer networks. Moreover, their ring structures can afford polymers with high glass transition temperatures. To develop epoxy resins containing sustainably sourced feedstocks, we designed and synthesized trehalose- and β -cyclodextrin-based carboxylic acid hardeners for epoxy resins and examined the thermal, mechanical, and adhesive properties of the resulting materials. Trehalose and β -cyclodextrin were succinylated with excess succinic anhydride, and the resulting carboxylic acid hardeners formed homogeneous mixtures with trimethylolpropane triglycidyl ether (TTE) in different carboxyl–epoxide ratios. The cured resins were found to be thermally stable ($T_{d5} > 300$ °C) and display high Young's moduli of up to 1.4 and 1.8 GPa with mechanical strengths of 47 and 64 MPa for the trehalose- and β -cyclodextrin-based epoxy resins, respectively. Preliminary adhesion tests showed that the cured resins exhibit excellent lap-shear strengths of 3600 and 2100 psi, respectively. The resins were also degradable into water-soluble components in both aqueous acidic and basic solutions but were relatively stable from hydrolysis in neutral aqueous conditions. These results imply that this novel class of hardeners are promising feedstocks for renewable high performance epoxy resins.

INTRODUCTION

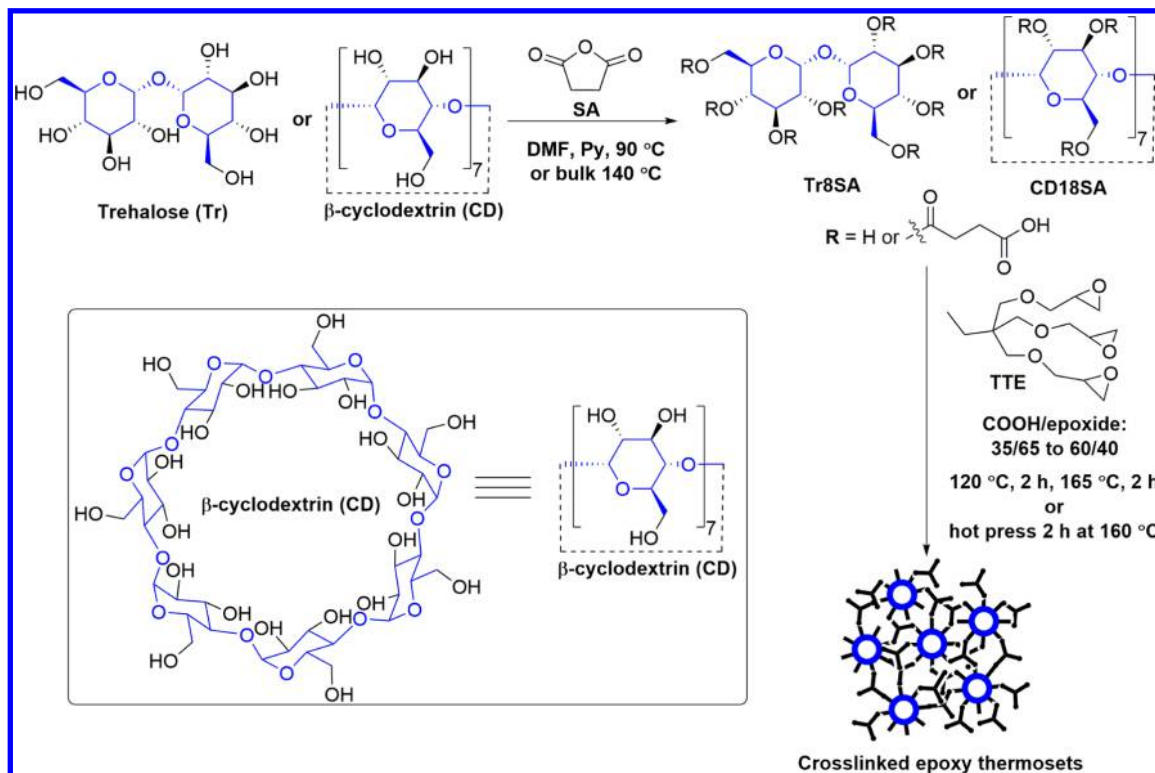
Epoxy resins are a unique class of high-performance thermoset materials, which upon curing leads to irreversibly cross-linked materials with outstanding attributes. In particular, these materials are known for their high mechanical strength, excellent adhesion to a variety of substrates, and high thermal and chemical resistance.^{1,2} Unfortunately, the monomeric precursors of current epoxy resins are obtained from non-renewable petroleum-based raw materials. Additionally, with regards to the human health and environmental safety, sustainable polymeric materials from natural sugar feedstocks have drawn significant attention among academic, industrial, and governmental communities.^{3–7} For example, the most popular epoxy monomer, bisphenol A diglycidyl ether, is derived from glycidylation of bisphenol A (BPA) and is used in ~90% of all industrial epoxy resins.⁸ However, the detrimental public health and environmental effects of trace BPA have been extensively reported, prompting research on alternative epoxy resin substitutes.⁹

Among the various strategies toward this goal, natural products such as carbohydrates offer opportunities to create new epoxy resin materials due to their sustainability, biodegradability, and natural abundance at low costs. The convenient combination of numerous hydroxyl group moieties and rigid ring backbone structures in carbohydrates can lead to highly functionalized monomers and allow highly cross-linked networks with high glass transition temperature (T_g) values.^{10,11} For instance, isosorbide, which contains two cis-fused tetrahydrofuran rings,¹² has been transformed into thermosetting epoxy resins via glycidylation with comparable thermal and mechanical properties to BPA-based polymers.^{13–16} Additionally, Liu et al. have synthesized an epoxy resin from 2,5-furandicarboxylic acid and studied its curing kinetics with methylhexahydrophthalic anhydride and poly-

Received: August 25, 2016

Revised: October 19, 2016

Published: November 7, 2016

Scheme 1. Synthesis of Sugar-Derived Epoxy Resin Hardeners^a

^aTr: trehalose; CD: β -cyclodextrin; SA: succinic anhydride; Tr8SA: succinylated trehalose hardener with ~ 8 SA units; CD18SA: succinylated β -cyclodextrin hardener with ~ 18 SA units.

(propylene glycol)bis(2-aminopropyl ether) (D230).¹⁷ The cross-linked polymers displayed elevated T_g values and similar mechanical properties compared with those cured with diglycidyl ester of terephthalic acid. These results indicate that sustainably sourced epoxy resins can potentially compete with petroleum-based syntheses of epoxy resins.

Trehalose and β -cyclodextrin are interesting carbohydrates that can be either obtained from natural sources or prepared from the inexpensive enzymatic fermentation of starch.^{18–20} They are nonreducing sugars; therefore, unlike other saccharides, they will not readily hydrolyze or decompose against acid, base, and heat, and exhibit high biocompatibility when incorporated into polymers.²¹ Individually, trehalose has been converted to linear polymers through reversible addition–fragmentation chain transfer (RAFT) polymerization,²² acetalization reactions with dialdehyde compounds,^{23,24} and “click” reactions (including hydrosilylation,²⁵ Diels–Alder,²⁶ and azide–acetylene coupling reactions^{27–31}). Meanwhile, β -cyclodextrin is a cyclic oligosaccharide consisting of (α -1,4)-linked- α -D-glucopyranose units and contains a lipophilic cone-shaped cavity surrounded by a hydrophilic shell.³² For drug and gene delivery, linear polymers containing β -cyclodextrin moieties have been prepared using grafting-to³³ and polycondensation methods.^{32,34–36}

Recent efforts have been made to cross-link trehalose and β -cyclodextrin and exploit their unique properties. Photopolymerized films made from trehalose-incorporated networks exhibited high transparency and good biocompatibility but low tensile strengths and moduli.^{37,38} Bio-based trehalose hydrogels, prepared through thiol–ene photopolymerization and redox radical polymerization, can effectively encapsulate and stabilize a wide variety of enzymes due to hydrogen bonding

and exhibit controlled and prolonged protein release behavior.^{39,40} β -Cyclodextrin-based cross-linked polymers have been extensively studied for inclusion-recognition applications, such as water pollutant adsorbent, due to the presence of cone-shaped cavities that allows organic molecule capture.^{41,42} For example, Alsbaee et al. recently reported a porous β -cyclodextrin-based cross-linked polymer that exhibited exceptional removal efficiency of organic micro-pollutants from water with regeneration ability.⁴³

To the extent of our knowledge, examples are lacking of thermosetting epoxy resin polymers from trehalose and β -cyclodextrin for applications such as plastics and adhesives. To this end, we report the facile synthesis of carboxylic acid-functionalized trehalose and β -cyclodextrin monomers as new bio-based hardeners for epoxy resins. We hypothesized that the multiple hydroxyl groups and rigid ring structure displayed by trehalose and β -cyclodextrin will offer rigidity and strong mechanical behavior to the resulting materials. Both trehalose and β -cyclodextrin were modified with succinic anhydride (SA), a sustainable derivative of starch and sugar, and the resulting hardeners were formulated with trimethylolpropane triglycidyl ether (TTE) at different ratios to study the impact of composition on the thermal and mechanical properties of the final thermally cured structures. The cross-linked polymers displayed high mechanical strength and are degradable under both acidic and basic conditions. The synthesized epoxy resins exhibited high adhesion shear strength, indicating the potential application of these carbohydrates in high-end adhesives.

RESULTS AND DISCUSSION

Hardener Synthesis. The multiple hydroxyl groups of anhydrous trehalose (Tr) and β -cyclodextrin (CD) were

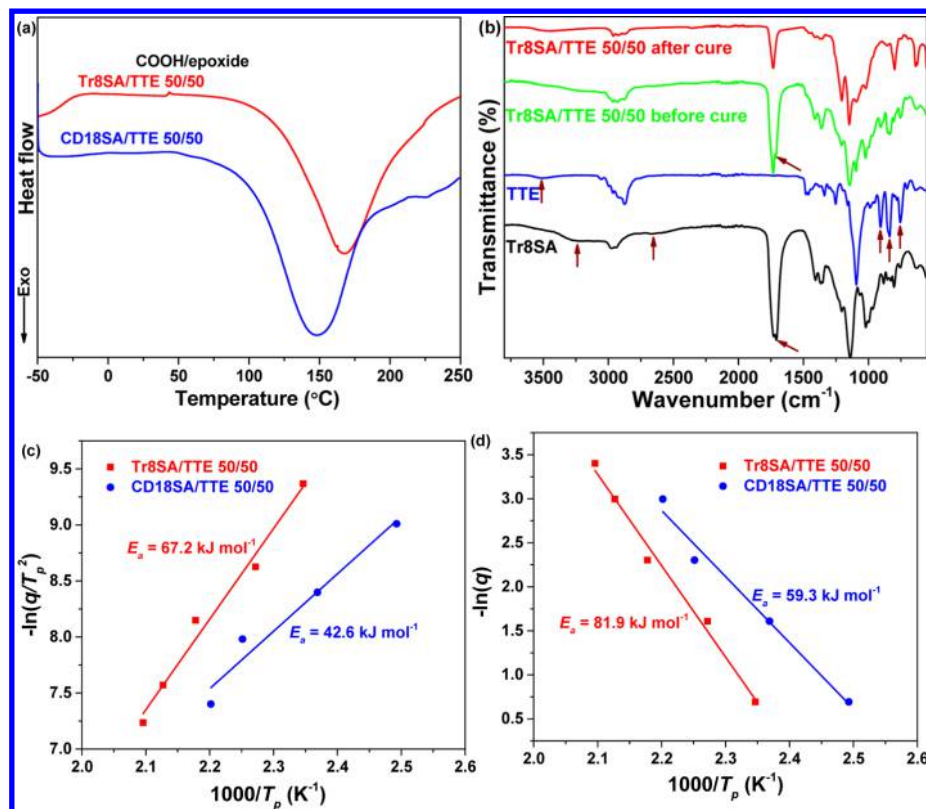


Figure 1. (a) DSC curing thermograms of Tr8SA/TTE and CD18SA/TTE (50/50, 5 °C min⁻¹) under nitrogen. (b) FT-IR spectra of Tr8SA, TTE, and Tr8SA/TTE (50/50) before and after thermal curing (arrows denote peaks of interest to support reaction conversion). (c) Linear plot of $-\ln(q/T_p^2)$ versus $1/T_p$ based on Kissinger's equation. (d) Linear plot of $\ln q$ versus $1/T_p$ based on Ozawa's equation.

esterified with excess succinic anhydride (SA) in dimethylformamide (DMF) in the presence of pyridine. The two carboxylic acid hardeners, Tr8SA and CD18SA (Scheme 1), were obtained in about 77% yield. The substitution degree and chemical structure of the two hardeners from Tr and CD were characterized by ¹H NMR and mass spectrometry. As shown in Figure S1 (Supporting Information), hardener Tr8SA prepared in DMF had an average substitution degree of 7.5, in good agreement with the mixture of 6–8 SA units per trehalose by mass spectrometry. With the exception of the anomeric proton, all other protons from trehalose shift downfield within the typical chemical shift range (4–5.8 ppm) of the ester in agreement with previous reports.^{44,45} Similarly, hardener CD18SA prepared in DMF had an average substitution degree of 18 (Figure S2) per CD unit. Elongating the reaction time did not further increase the substitution degree of SA unit for both Tr and CD. However, the synthesis of both Tr8SA and CD18SA required the use of DMF and pyridine solvents, which decreases the sustainability of the designed hardeners for preparing sustainable epoxy resin polymers. Therefore, the synthesis of the two hardeners was further optimized by using an excess of SA as both a reagent and the reaction solvent by heating to 140 °C; this reaction was thus performed without any additional solvents or base in less than 8 h and thus provided a greener chemical process to obtain the hardeners. Because succinic acid is highly aqueous soluble, the excess of SA was hydrolyzed to succinic acid by adding a mixture of acetone and water with heating to promote a facile purification of the synthesized hardeners. The ¹H NMR spectra (Figures S3 and S4) clearly show that both hardeners from the improved synthesis have average SA substitution degrees of 7.7 and 20

per trehalose and β -cyclodextrin, respectively, comparable to those prepared from the less-green method using DMF/pyridine. Thus, the synthesis of sugar-derived hardeners was optimized via a simple and green process without the use of toxic solvents to move forward to prepare the thermosetting epoxy resins.

Thermal Curing Behavior and Bulk Polymerization of Epoxy Resins. Carboxylic acid hardeners can polymerize with epoxides via ring-opening to form polyesters upon heating. Therefore, the two synthesized hardeners were formulated with TTE, an ideal reactive and high functional epoxy resin diluent for preparing adhesives and coating materials with improved flexibility and toughness.⁴⁶ The reactions were completed in different molar ratios (35/65 to 60/40) of $-COOH$ /epoxide and formed homogeneous epoxy formulations (Scheme 1). Figure 1a shows the differential scanning calorimetry (DSC) thermograms of Tr8SA/TTE and CD18SA/TTE at 50/50 ratios with a heating rate of 5 °C min⁻¹. Both epoxy resin systems display a single exothermic peak at around 170 and 150 °C for Tr8SA/TTE and CD18SA/TTE, respectively. These exothermic peaks can be attributed to the ring-opening of the epoxides in TTE by the COOH groups of the hardeners at elevated temperatures. Under the same curing conditions, the peak temperature detected by the nonisothermal DSC curve can be used to evaluate the reactivity of the reagents in the curing reaction. The peak temperature of Tr8SA/TTE is about 20 °C higher than that of CD18SA/TTE (Figure 1a and Figures S5 and S6), indicating the lower reactivity of Tr8SA.⁴⁷ In practical applications, epoxy resins are cured at constant temperatures, and a postcure may be applied at a higher temperature for optimized polymer properties. As indicated by

DSC isothermal scans (Figure S7), the exotherm of bulk polymerizations disappeared after approximately 20 min, indicating the fast curing rate for the two epoxy resin systems. Thus, a temperature of ~ 170 and ~ 160 $^{\circ}\text{C}$ was selected for bulk polymerization of the formulated epoxy resin Tr8SA/TTE and CD18SA/TTE, respectively. Fourier transform infrared (FT-IR) spectra of the resin mixture (Tr8SA/TTE, 50/50) before and after cure were recorded as shown in Figure 1b. As shown in Figure 1b, the broad peak at 3460 cm^{-1} after thermal curing indicates the presence of hydroxyl groups from ring-opening of epoxide groups after polymerization. The broad peak in the range of $3300\text{--}2500\text{ cm}^{-1}$ and the adsorption band at 1700 cm^{-1} from the $-\text{COOH}$ groups of hardeners and the peaks from the epoxide rings at 910, 835, and 750 cm^{-1} completely disappeared after thermal curing. These results indicate the successful ring-opening of the epoxides by $-\text{COOH}$ groups to form cross-linked polymers (Figures S8–S10).

It should be noted that the curing reactivity of epoxy resins is greatly affected by the heating rate of the DSC experiments and the peak curing temperature shifts with different heating rates (for non-isothermal curing). Therefore, the activation energy (E_a) of the thermal curing reactions was determined from the peak temperatures at different heating rates of dynamic DSC scans by both Kissinger's⁴⁸ and Ozawa's⁴⁹ methods. Based on Kissinger's theory, the activation energy can be calculated from the peak temperatures at different heating rates using the Kissinger equation:

$$-\ln(q/T_p^2) = E_a/RT_p - \ln(AR/E_a) \quad (1)$$

where q is the heating rate of DSC thermal curing scans, T_p is the exothermic peak temperature, E_a is the activation energy, R is the gas constant ($8.314\text{ J mol}^{-1}\text{ K}^{-1}$), and A is the pre-exponential factor. A plot of $-\ln(q/T_p^2)$ versus $1/T_p$ allows determination of the apparent activation energy from the slope of the linear fit.⁴⁸ Moreover, Ozawa's method can also be used to calculate the activation energy, which is expressed by eq 2:

$$\ln q = -1.052E_a/RT_p + \ln(AE_a/R) - \ln F(x) - 5.331 \quad (2)$$

where $F(x)$ is a conversion-dependent term. Therefore, E_a could be calculated from the slope of a linear fitting plot of $\ln q$ versus $1/T_p$.⁴⁹

The linear fits of Kissinger's equation (eq 1) as well as Ozawa's equation (eq 2) are shown in Figures 1c and 1d, respectively, for Tr8SA/TTE 50/50 and CD18SA/TTE 50/50. Accordingly, the E_a values of the thermal curing reactions for a sample of Tr8SA/TTE 50/50 were calculated as 67.2 kJ mol^{-1} (Kissinger method) and 81.9 kJ mol^{-1} (Ozawa method). These activation energy values were much higher than the calculated E_a values, 42.6 kJ mol^{-1} (Kissinger method) and 59.3 kJ mol^{-1} (Ozawa method) for the sample of CD18SA/TTE 50/50. These results suggest that CD18SA has a higher reactivity than that of Tr8SA toward thermal curing with TTE,⁵⁰ which agreed well with the results from the nonisothermal DSC curves as discussed above (Figure 1a).

Thermal Properties of the Cured Epoxy Thermosets. The formulation of the two hardeners with TTE afforded homogeneous viscous liquid resins from the Tr8SA/TTE hardener and solid resins from the CD18SA/TTE hardener. The resulting epoxy resins were thermally cured, and their thermal stability under nitrogen was investigated by thermog-

ravimetric analysis (TGA) (Figure 2a and Figure S11). The degradation temperatures at 5% weight loss (T_{d5}) of the cured

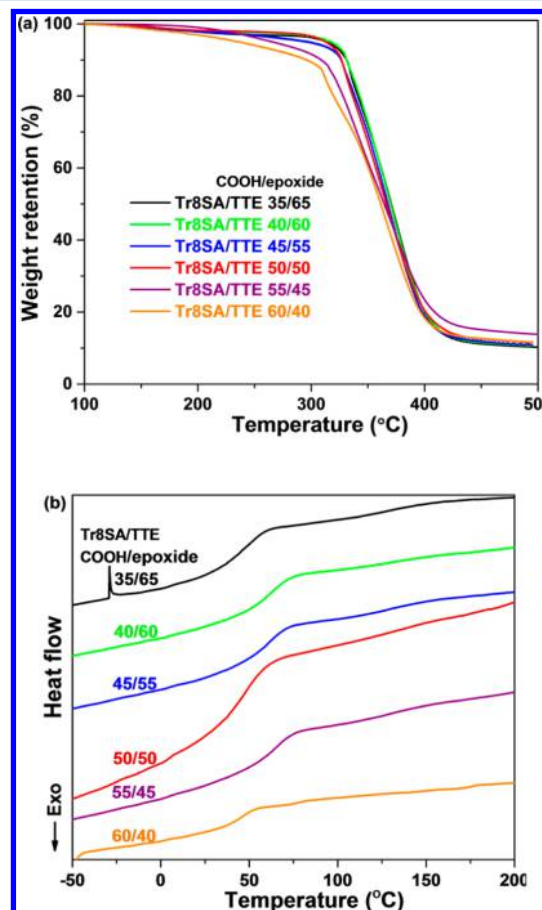


Figure 2. (a) TGA curves of cured Tr8SA/TTE at heating rate of $10\text{ }^{\circ}\text{C min}^{-1}$ under nitrogen and (b) DSC thermograms (second heating) of cured Tr8SA/TTE at different ratios with a heating rate of $10\text{ }^{\circ}\text{C min}^{-1}$ under nitrogen.

materials were around $300\text{ }^{\circ}\text{C}$, which was about $100\text{ }^{\circ}\text{C}$ higher than those of either hardeners or TTE alone (Figure S11). The much higher thermal stability of the materials clearly suggests the formation of the cross-linked networks. The T_{d5} of the polymers generally decreased with increasing hardener content. This might be due to the lower cross-linking density of the network formed at higher $-\text{COOH}$ /epoxide ratios (unreacted $-\text{COOH}$ groups can remain in the polymer). However, the excess of TTE at lower $-\text{COOH}$ /epoxide ratios can potentially still participate in the polymerization through primary or secondary hydroxyl groups from ring-opening of TTE.¹⁴ The T_g of the resulting polymers from DSC measurements (Figure 2b and Figure S12) shifted to higher temperatures and then decreased as the ratios of $-\text{COOH}$ /epoxide increased from 35/65 to 60/40. Tr8SA/TTE (45/55) and CD18SA/TTE (50/50) exhibited T_g values of 63 and $83\text{ }^{\circ}\text{C}$, respectively. This indicates that tuning the mixing ratio of the hardeners and epoxy in the resins can greatly affect the cross-linking reaction and the resulting thermal and mechanical properties. We measured the swelling ratio and gel fraction of the polymers obtained in tetrahydrofuran (THF, a good solvent for TTE, hardeners, and linear polyesters), which is shown in Table 1. These results reveal that both monomers participated in polymerization, and a higher cross-link density was achieved at equimolar

Table 1. Characterization Data for Cross-Linked Thermosets

polymer	swelling ratio ^a	gel fraction ^a	T _{ds} ^b (°C)	T _g ^c (°C)
Tr8SA/TTE 35/65	1.38 ± 0.03	0.896 ± 0.021	310	48
Tr8SA/TTE 40/60	1.25 ± 0.05	0.918 ± 0.015	317	63
Tr8SA/TTE 45/55	1.29 ± 0.08	0.926 ± 0.014	300	63
Tr8SA/TTE 50/50	1.30 ± 0.04	0.961 ± 0.019	300	51
Tr8SA/TTE 55/45	1.34 ± 0.07	0.854 ± 0.013	266	57
Tr8SA/TTE 60/40	1.46 ± 0.06	0.959 ± 0.025	238	45
CD18SA/TTE 35/65	1.15 ± 0.04	0.973 ± 0.013	317	49
CD18SA/TTE 40/60	1.10 ± 0.01	0.980 ± 0.013	322	52
CD18SA/TTE 45/55	1.15 ± 0.01	0.975 ± 0.016	300	64
CD18SA/TTE 50/50	1.05 ± 0.01	0.979 ± 0.009	299	83
CD18SA/TTE 55/45	1.16 ± 0.02	0.931 ± 0.016	302	56
CD18SA/TTE 60/40	1.09 ± 0.05	0.971 ± 0.012	296	51

^aDetermined by immersing the samples in THF for 48 h, the wet weight was measured for the swelling ratio calculation. The dry weight was measured for the gel fraction calculation after drying the samples at 50 °C under high vacuum. ^bTemperatures at 5% weight loss were determined using TGA. ^cTemperatures were determined by performing DSC at 10 °C min⁻¹ under nitrogen.

—COOH/epoxide ratios. It was found that the CD18SA/TTE resin system formed a network with higher cross-linking density, as indicated by the lower swelling ratios and higher gel fractions. Also, the —COOH/epoxide ratio did not appear to have much of an effect on the gel fraction of the CD18SA/TTE polymers. While the rigidity and cross-linking density did not affect the thermal stability and swelling ratios and gel fractions of polymer networks, CD18SA/TTE resin systems displayed a higher T_g than the analogous Tr8SA/TTE polymers. This is likely due to the greater structural rigidity and functionality of β -cyclodextrin. Collectively, these results indicate the greater rigidity of β -cyclodextrin compared to trehalose. Both T_{ds} and T_g of the synthesized epoxy polymers are comparable to the reported values (~250–300 °C for T_{ds} and ~30–90 °C for T_g) of other sustainably sourced epoxy thermosets containing sugar-derived moieties, including isosorbide, furandicarboxylic acid, itoconic acid, starch, and eugenol.^{14,17,50–52} When compared to BPA-based epoxy resins, all of these sustainable epoxy thermosets generally display slightly lower thermal stability. This is likely due to the aliphatic network common in many sugar-derived sustainable epoxy thermosets. Indeed, the mechanical performance presented herein indicates the potential of carbohydrates for preparing bio-based epoxy resins.

Mechanical Properties of the Cured Epoxy Thermosets. The homogeneous viscous liquid resins from Tr8SA/TTE were loaded onto rubber molds and completely dried under high vacuum to remove residual acetone and avoid bubbling during thermal curing. The liquid resins were transferred into a convection oven and were cured via a pre-curing/post-curing process to afford light yellow or slightly dark yellow tensile bars. The solid CD18SA/TTE-based epoxy resins were directly cured with a hot press to yield light yellow tensile bars for mechanical measurements. In general, the chemical structure of the hardeners and epoxy has a significant effect on the cross-linking density of the polymer network and hence influences the mechanical properties. As shown in Figure 3a and Table 2, thermosetting polymers of Tr8SA/TTE exhibited a high tensile strength of up to 47 MPa with a strain of 16%. Because of the more rigid structure and higher cross-linking density of the β -cyclodextrin hardeners, cured CD18SA/TTE epoxy resins showed a much higher tensile strength of up to 64 MPa. The

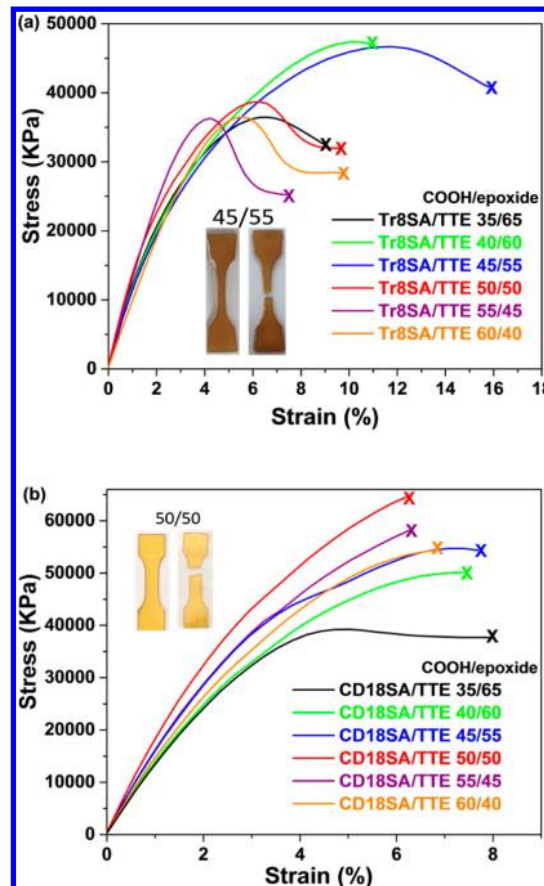


Figure 3. Representative stress-strain curves for cured (a) Tr8SA/TTE and (b) CD18SA/TTE at different ratios by tensile testing from at least five polymer tensile bars. Inset images are the representative tensile bars before and after tensile testing.

Table 2. Tensile and Thermal Mechanical Characterization for Cross-Linked Thermosets

polymer	Young's modulus ^a (GPa)	tensile strength ^a (MPa)	strain at break ^a (%)	storage modulus ^b (GPa)
Tr8SA/TTE 35/65	1.21	36	8.9	— ^c
Tr8SA/TTE 40/60	1.19	47	12	1.03
Tr8SA/TTE 45/55	1.35	47	16	0.936
Tr8SA/TTE 50/50	1.37	39	9.7	0.710
Tr8SA/TTE 55/45	1.33	36	6.7	— ^c
Tr8SA/TTE 60/40	0.986	36	9.7	— ^c
CD18SA/TTE 35/65	1.34	38	7.9	— ^c
CD18SA/TTE 40/60	1.39	50	7.4	— ^c
CD18SA/TTE 45/55	1.57	55	7.7	1.48
CD18SA/TTE 50/50	1.81	64	6.3	1.21
CD18SA/TTE 55/45	1.64	63	8.6	1.20
CD18SA/TTE 60/40	1.48	54	6.8	— ^c

^aDetermined from stress-strain tests and averaged from at least five tensile bars. ^bDetermined from dynamic mechanical analysis (DMA) at 20 °C with torsion geometry. ^cNot tested by DMA.

cured CD18SA/TTE epoxy resins were slightly more brittle as evidenced by the immediate fracture without typical plastic deformation in stress-strain curves (Figure 3b) as compared to the Tr8SA/TTE samples.^{53,54} Both epoxy resin systems have relatively high Young's moduli of up to ~1.4 and 1.8 GPa at —COOH/epoxide ratios at 45/55 and 50/50, respectively,

indicating the glassy nature of the epoxy polymers at room temperature. The high mechanical strength of these systems could be attributed to the presence of the rigid sugar rings and highly cross-linked network. Both tensile strength and Young's moduli of the resulting polymers increased and then decreased as the ratios of $-\text{COOH}/\text{epoxide}$ increased from 35/65 to 60/40. The highest tensile strength and Young's moduli values were obtained at $\sim 50/50$ ratio of $-\text{COOH}/\text{epoxide}$, indicating formation of the strongest cross-linked network (Table 2). Although the mechanical performance of both Tr8SA/TTE and CD18SA/TTE polymers are a slightly lower when compared to petroleum-derived feedstocks, this result is likely due to the presence of the aliphatic epoxy structure. However, it should be noted that the mechanical performance is comparable to other epoxy thermosets consisting of sugar derivatives isosorbide and furan moieties that offer values of $\sim 30\text{--}80$ MPa for tensile strength and $\sim 1.4\text{--}3.0$ GPa for Young's modulus.^{14,17}

Dynamic Mechanical Properties of Cured Epoxy Thermosets.

To study the variation of mechanical properties at elevated temperatures and the transition between glassy and rubbery states of the epoxy resins, dynamic mechanical analysis (DMA) experiments were conducted from -50 to 160 $^{\circ}\text{C}$. As shown in Figure 4, as the temperature increased, all epoxy thermosets demonstrated three regions of viscoelasticity: (i) the glassy state, (ii) the leathery state, and (iii) the rubbery state. In the glassy state, the storage moduli of all examined Tr8SA/TTE epoxy resins exhibited little change at ~ 1 GPa,

while the CD18SA/TTE-based epoxy resins exhibited moderately higher storage moduli around 1.2–1.4 GPa. As the temperature increased, the storage moduli decreased gradually followed by a large storage modulus drop of 1–2 orders of magnitude due to the polymer chain relaxation at the glass transition. We observe that the CD18SA/TTE epoxy resins exhibited a much slower storage moduli drop over a range of ~ 70 $^{\circ}\text{C}$ than that of the Tr8SA/TTE resins over a range of only ~ 30 $^{\circ}\text{C}$. These results further confirm the higher cross-linking density and rigidity of the β -cyclodextrin structure in the CD18SA/TTE epoxy resin polymers. The higher cross-linking density can retard and restrict the polymer chain mobility and subsequently lead to a much slower change of storage moduli with heating.^{55,56} The damping property ($\tan \delta$) of epoxy resins are shown in Figures S13 and S14. The CD18SA/TTE epoxy resins exhibited much broader $\tan \delta$ peaks, indicating the presence of a highly cross-linked polymer network. However, the Tr8SA/TTE polymers have much higher $\tan \delta$ intensity due to their lower cross-linking density.⁵⁷ This demonstrates the greater toughness and ability to effectively avoid material failure of the Tr8SA/TTE systems as they can more effectively absorb and dissipate energy through chain segmental motions with applied force, such as tension, shock, or vibration.^{58,59}

Preliminary Adhesion Strength of the Cured Epoxy Thermosets.

Epoxy resins in high-performance structural and specialty composite applications hinge on the ease of processability, high tensile strength, low shrinkage, and excellent adhesion to various substrates.^{1,2} Hence, the adhesion lap shear strengths of the prepared epoxy resins were measured to evaluate their potential application as adhesives. Two epoxy resins with the highest tensile strength, Tr8SA/TTE 45/55 and CD18SA/TTE 50/50, were selected for lap shear adhesion testing. The single-lap-joint specimens were prepared by loading the appropriate amount of completely dried liquid or solid epoxy resin onto stainless steel strips followed by thermal curing. The force–extension curves (Figures S15 and S16) showed that the Tr8SA/TTE 45/55 resisted a much higher force loading than CD18SA/TTE 50/50. For more accurate comparison, their adhesion strength was calculated from force–extension curves and plotted in Figure 5. Tr8SA/TTE 45/55 and CD18SA/TTE 50/50 have high lap shear adhesion strength values of ~ 3600 and 2100 psi, respectively. For example, the lap shear strength of Tr8SA/TTE 45/55 polymer is similar to the manufacturer-claimed adhesion strength of

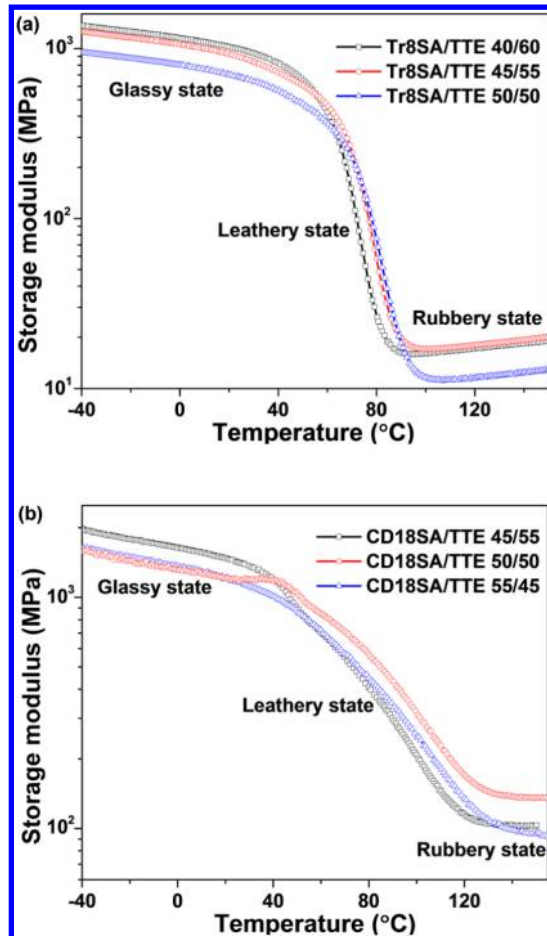


Figure 4. Storage modulus–temperature curves for the cured (a) Tr8SA/TTE and (b) CD18SA/TTE thermosets by DMA.

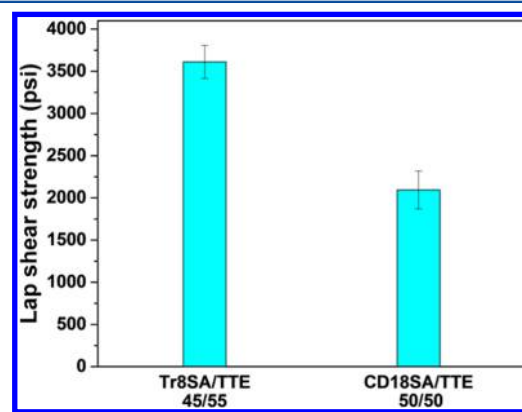


Figure 5. Adhesion lap shear strength of cured Tr8SA/TTE (45/55) and CD18SA/TTE (50/50) at different ratios. Error bars represent the standard deviation of the mean from at least three specimens.

Loctite two-part epoxy adhesives D609 (2900 psi) and 615 (3800 psi) used for multiple surface bonding, which indicates its potential applications as a strong adhesive. The observed high lap-shear adhesion strength could be partially attributed to the high content of hydroxyl groups after thermal curing, which appear to have a strong adhesive attraction to the polar metallic surface of the stainless steel.^{60–62} Although the Tr8SA/TTE 45/55 sample exhibited lower tensile strength than the CD18SA/TTE 50/50 sample, the Tr8SA/TTE 45/55 demonstrated much higher adhesion strength, which could be attributed to its higher damping property for energy adsorption and dissipation and its less brittle nature.⁶³ The bonding area after pulling the specimen apart was examined as shown in Figure S17; the residual adhesive remained on one adherend surface indicating adhesive failure, and the adhesive strength at the bonding interface is weaker than the tensile strength of adhesive.

Hydrolytic Degradation of the Prepared Thermosets.

The hydrolytic stability of the cured epoxy resins in basic, neutral, and acidic aqueous environments was evaluated by monitoring the insoluble mass of polymers over time. As shown in Figure 6a and Figure S18, both the trehalose- and β -cyclodextrin-based epoxy resin samples quickly degraded in 1 M NaOH, resulting in completely water-soluble degradation products over a varying time period of several hours to 1.5 days. To further investigate the degradation products, two polymer samples were completely degraded in 1 M NaOD/D₂O and analyzed by ¹H NMR spectroscopy. As shown in Figure S21, the degraded products consisted of trehalose, β -cyclodextrin, the ring-opened product of TTE, and disodium succinate, indicating complete degradation of the cross-linked polymer network to environmentally benign products. In acidic conditions, the final networked materials exhibit slightly different behavior; in 1 M HCl, the cured polymers first rapidly swell about 5–10% of the original volume, after which gradual degradation occurs from day 15 and 24. All samples were found to completely degrade to water-soluble components after 50–90 days (Figure 6b and Figure S19). It is well-known that the acid-catalyzed hydrolysis of esters is an equilibrium process and is much slower than that under basic conditions.⁶⁴ In neutral aqueous conditions, the epoxy polymers were found to swell, where they reached a maximum mass in a time frame of about 1–10 days for the Tr8SA/TTE and CD18SA/TTE polymers, respectively (Figure 6c and Figure S19). No weight loss or further swelling occurred over the test period of 70–90 days. These results indicate that the synthesized epoxy thermosets can be quickly hydrolyzed via a triggered mechanism under either basic or acidic conditions to their starting materials or derivatives. Indeed, the degraded products from these structures are more environmentally benign compared to those from traditional epoxy resin thermosets, such as BPA and bisphenol S.

CONCLUSION

We have reported the preparation of two new sustainably sourced hardeners based on trehalose and β -cyclodextrin, which can be used to formulate strong bio-based epoxy resin polymers. The preparation of the epoxy hardeners was optimized with high yields via a green methodology by eliminating the need for organic solvents and bases. The prepared hardeners can be formulated with TTE to afford homogeneous epoxy resins. DSC experiments revealed that the resulting epoxy resins can be thermally cured at \sim 160–170 °C,

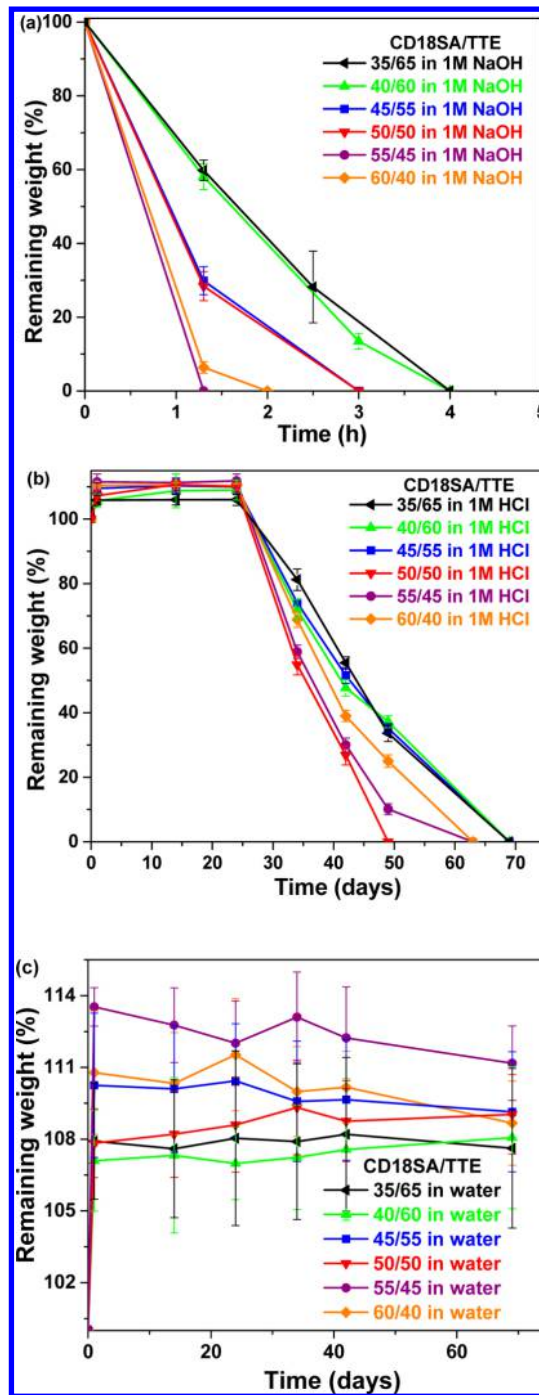


Figure 6. Hydrolytic degradation/stability profile of cured CD18SA/TTE at different ratios in (a) 1 M NaOH, (b) 1 M HCl, and (c) water.

and the resulting cured epoxy thermosetting polymers have high thermal stability up to about 300 °C. Both tensile testing and thermal mechanical analysis suggest that CD18SA/TTE-based epoxy resins display higher mechanical performance (64 MPa for tensile strength and 1.8 GPa for Young's modulus) than Tr8SA/TTE-based epoxy polymers (47 MPa for tensile strength and 1.4 GPa for Young's modulus). However, Tr8SA/TTE-based epoxy polymer had much higher adhesion lap-shear strength of 3600 psi than CD18SA/TTE-based epoxy resins with adhesion lap-shear strength of 2100 psi. The sugar-based epoxy polymers are degradable to water-soluble components in basic solution within 1.5 days and also completely hydrolyze in

acidic aqueous conditions in a slow manner. Yet, the epoxy resins are resistant to degradation in neutral aqueous conditions over a testing period of 90 days. These results imply that this class of novel bio-based hardeners holds great promise for preparing sustainable high performance epoxy resins with high mechanical and adhesion strength that can be hydrolyzed to environmentally benign products in a controllable manner.

■ EXPERIMENTAL SECTION

Materials. All chemicals and solvents were purchased from Aldrich and used without further purification unless otherwise noted. Anhydrous trehalose (Tr) was purchased from Acros Organics. Food grade trehalose (Tr) was purchased from Swanson Health Products. Food grade β -cyclodextrin (CD) was supplied by Wacker Chemie AG. Succinic anhydride (SA) was purchased from Alfa Aesar and used without further purification. Dialysis membranes were obtained from Spectrum Laboratories, Inc. Dry dimethylformamide (DMF) was obtained using an MBRAUN MB solvent purification system manufactured by M. Braun Inert gas-System GmbH (Garching, Germany) using HPLC grade solvent.

Characterization. ^1H NMR spectroscopy experiments were performed on a Bruker Avance III HD 500 spectrometer at 500 MHz. FT-IR spectra were obtained using a Bruker Alpha Platinum ATR spectrometer. High resolution mass spec was performed using a Bruker Bio-TOF II in positive mode ESI. TGA was performed on a TA Instruments Q500 at a heating rate of $10\text{ }^\circ\text{C min}^{-1}$ under a nitrogen flow of 60 mL min^{-1} in a temperature range from 25 to $520\text{ }^\circ\text{C}$. Differential scanning calorimetry (DSC) measurements were carried out using a TA Instruments Discovery DSC under a nitrogen atmosphere. T_g values were determined on the second heating at a heating rate of $10\text{ }^\circ\text{C min}^{-1}$. The curing behavior was measured by DSC at heating rates of 2, 5, 10, 20, and $30\text{ }^\circ\text{C min}^{-1}$. Tensile testing was performed using a Minimat Tensile Tester on samples with a dog-bone geometry (typical gauge dimensions $14 \times 1.30 \times 1.20\text{ mm}$ or $14 \times 3.0 \times 0.50\text{ mm}$) at a free crosshead rate of 5 mm min^{-1} . The thermal dynamic mechanical analysis of the cure samples was conducted on a TA Instruments ARES-G2 rheometer with a rectangular torsion geometry. Adhesive lap shear testing was conducted according to ASTM D1002 in tension mode on an Instron 5966 universal testing system with a 10 kN load cell at a free crosshead rate of 5 mm min^{-1} .

Synthesis of Hardeners. *Synthesis of Trehalose-Based Hardener (Tr8SA) in DMF with Pyridine.* In a 250 mL round-bottom flask, anhydrous Tr (5.14 g , 15.0 mmol) was added and stirred in 100 mL of anhydrous DMF at $90\text{ }^\circ\text{C}$ until completely dissolved to give a clear solution. SA (15.0 g , 150 mmol), pyridine (20.0 mL), and DMAP (0.916 g , 0.625 equiv to hydroxyl groups) were added into the mixture, and the resulting solution was stirred for 48 h at $90\text{ }^\circ\text{C}$. The flask was taken out of the oil bath and rotavaped to remove half of the DMF solvent, and 500 mL of ethyl acetate was added to dissolve the product. The resulting mixture was transferred to a 1 L separatory funnel and extracted with 2 M HCl with brine ($1 \times 300\text{ mL}$, $2 \times 100\text{ mL}$) and deionized water until all of the succinic acid was removed from the mixture. The organic layer was decolorized by activated charcoal, dried with anhydrous sodium sulfate, and concentrated under vacuum to give a light yellow foamy solid; 13.2 g , 77.0% . ^1H NMR (acetone- d_6 , 500 MHz) δ_{ppm} : $5.80\text{--}5.56\text{ (m, 2H)}$, $5.53\text{--}5.26\text{ (m, 2H)}$, $5.25\text{--}4.97\text{ (m, 4H)}$, $4.45\text{--}3.93\text{ (m, 6H)}$, $2.90\text{--}2.38\text{ (m, 30.7H)}$. ESI-MS (m/z) Calcd for $\text{C}_{36}\text{H}_{46}\text{NaO}_{29}$ ($\text{M} + \text{Na}^+$; Tr6SA): 965.20 , found: 965.09 . $\text{C}_{40}\text{H}_{50}\text{NaO}_{32}$ ($\text{M} + \text{Na}^+$; Tr7SA): 1065.22 , found: 1065.08 . $\text{C}_{44}\text{H}_{54}\text{NaO}_{35}$ ($\text{M} + \text{Na}^+$; Tr8SA): 1165.23 , found: 1165.08 .

Synthesis of β -Cyclodextrin-Based Hardener (CD18SA) in DMF with Pyridine. Anhydrous CD (10.1 g , 8.90 mmol) was weighted and stirred in 150 mL of anhydrous DMF in a 250 mL round-bottom flask at $90\text{ }^\circ\text{C}$ until completely dissolved to give a clear solution. SA (37.4 g , 374 mmol), pyridine (50.0 mL), and DMAP (1.40 g , 0.625 equiv to hydroxyl groups) were added, and the resulted mixture was stirred for another 48 h at $90\text{ }^\circ\text{C}$. After removal of DMF, the mixture was dissolved in acetone and purified by dialysis (tubing MWCO: 1000 Da) against diluted HCl solution ($\sim 0.3\text{ M}$) and DI water for 4 days .

The dialysis solution was periodically replaced with fresh DI water. The retained product inside the dialysis tubing was collected and dissolved in acetone. After decolorization by activated charcoal, the acetone solution was filtered, and the product was isolated after drying under vacuum. A light yellow foamy solid was afforded, 22.0 g , 76.4% . ^1H NMR (acetone- d_6 , 500 MHz) δ_{ppm} : $5.82\text{--}3.50\text{ (m, 49H)}$, $3.31\text{--}2.20\text{ (m, 72.3H)}$.

Improved Synthesis of Hardeners. *Bulk Synthesis of Trehalose-Based Hardener (Tr8SA) without Using DMF Solvent.* Oven-dried ($120\text{ }^\circ\text{C}$, 2 h) food grade trehalose (Tr, 5.14 g , 15.0 mmol), SA (15.0 g , 150 mmol), and DMAP (0.250 g , 0.125 equiv to hydroxyl groups) were deposited into an oven-dried 100 mL round-bottom flask. The resulting mixture was stirred for 8 h at $140\text{ }^\circ\text{C}$, and the flask was taken out of the oil bath followed by the careful addition of a mixture of acetone–water ($\sim 2:1$) until the mixture was dissolved under heating. The solution was mixed with 800 mL of ethyl acetate, and the resulted mixture was transferred to a 1 L separatory funnel and extracted with 2 M HCl with brine ($2 \times 100\text{ mL}$) and DI water until there was no succinic acid left in the mixture. The organic layer was dried with anhydrous sodium sulfate and concentrated under vacuum to give a light yellow foamy solid; 13.4 g , 78.8% . ^1H NMR (acetone- d_6 , 500 MHz) δ_{ppm} : $5.79\text{--}5.56\text{ (m, 2H)}$, $5.55\text{--}5.27\text{ (m, 2H)}$, $5.26\text{--}4.88\text{ (m, 4H)}$, $4.50\text{--}3.89\text{ (m, 6H)}$, $2.93\text{--}2.31\text{ (m, 31.3H)}$. ESI-MS (m/z) Calcd for $\text{C}_{40}\text{H}_{50}\text{NaO}_{32}$ ($\text{M} + \text{Na}^+$; Tr7SA): 1065.22 , found: 1065.00 . $\text{C}_{44}\text{H}_{54}\text{NaO}_{35}$ ($\text{M} + \text{Na}^+$; Tr8SA): 1165.23 , found: 1165.00 .

Bulk Synthesis of β -Cyclodextrin-Based Hardener (CD18SA) without Using Solvent DMF. Oven-dried ($120\text{ }^\circ\text{C}$, 2 h) food grade β -cyclodextrin (CD, 7.41 g , 6.53 mmol), SA (27.4 g , 274 mmol), and DMAP (0.209 g , 0.125 equiv to hydroxyl groups) were weighted and deposited into an oven-dried 100 mL round-bottom flask equipped with a stir bar. The flask was put into a $140\text{ }^\circ\text{C}$ oil bath and stirred for 8 h . The resulting dark mixture was dissolved in a mixture of acetone–water ($\sim 2:1$) under heating and purified via dialysis (tubing MWCO: 1000 Da) against diluted HCl solution ($\sim 0.3\text{ M}$) and DI water for 96 h . The dialysate was collected and dissolved in acetone. After decolorization by activated charcoal and concentration under vacuum, a light yellow foamy solid was obtained; 14.0 g , 66.3% . ^1H NMR (acetone- d_6 , 500 MHz) δ_{ppm} : $5.73\text{--}3.60\text{ (m, 49H)}$, $3.20\text{--}2.40\text{ (m, 81H)}$.

Formulation of Epoxy Resins and Tensile Bar Preparation. The synthesized hardeners were formulated with trimethylolpropane triglycidyl ether (TTE) in different molar ratios of $-\text{COOH}$ /epoxide ($35/65$, $40/60$, $45/55$, $50/50$, $55/45$, and $60/40$) by a solvent blending method. Briefly, accurately weighted hardeners and TTE were put into a 20 mL scintillation glass vial followed by the addition of acetone to dissolve and mix the monomers. Acetone was then removed via rotavap at $30\text{ }^\circ\text{C}$, and the resulting epoxy resins were dried under high vacuum as either viscous liquids or solids and stored in a freezer for later use. The thermal curing of the resins was conducted in the following two methods based on the physical form of the formulated resins. (1) The viscous liquid epoxy resins from trehalose-based hardener was transferred into rubber silicone mold that contained a dog-bone shape and then dried under vacuum for 12 h at room temperature. Then, the epoxy resins were precured at $120\text{ }^\circ\text{C}$ for 2 h and postcured at $165\text{ }^\circ\text{C}$ for 2 h for further mechanical testing. (2) The solid epoxy resins from the β -cyclodextrin-based hardeners were loaded into a stainless steel mold with a dog-bone shape and cured at $\sim 160\text{ }^\circ\text{C}$ for 2 h in a hot press under a pressure of 3000 psi .

Hydrolytic Degradation. The degradation properties of the epoxy resins were examined in deionized (DI) H_2O , 1 M NaOH , and 1 M HCl and were evaluated as follows: Three parallel samples of polymer ($\sim 50\text{ mg}$, dog-bone shape) were immersed in the appropriate aqueous solution (5 mL) and allowed to sit undisturbed at room temperature. The samples were periodically removed, blotted dry, weighed, and reimmersed in the same solution. Degraded samples for NMR analysis were prepared by immersing the polymers in a solution of 1 M NaOD in D_2O until the mixture became homogeneous.

Swelling Ratio and Gel Fraction Measurement. Three parallel samples of cured polymers ($\sim 50\text{ mg}$, dog-bone shape) were weighed

(m_1) and immersed into 4 mL of THF for 48 h to remove the solubilized fraction. Then the wet weight (m_2) of the polymer samples was recorded for the swelling ratio calculation. After the wet samples were completely dried at 50 °C under high vacuum for 24 h, the dry weight (m_3) of polymer samples was recorded for the gel fraction calculation. The swelling ratio and gel fraction were calculated according [eqs 3](#) and [4](#).

$$\text{swelling ratio} = m_2/m_1 \quad (3)$$

$$\text{gel fraction} = m_3/m_1 \quad (4)$$

Lap Shear Adhesion Test. Lap shear strip specimens were machined from a stainless steel panel (type 316) with dimensions of 104 × 25.4 × 1.50 mm. All specimens were pretreated by soaking in concentrated sulfuric acid for 1 h followed by washing with deionized water, acetone, and dichloromethane. The completely dried epoxy resins samples (~80 mg) were weighed and uniformly applied over a bonding area of ~12.7 mm × 25.4 mm on steel specimens. Two 0.5 mm long stainless steel wires (diameter: 0.125 mm) were placed in the resin bonding area to ensure a uniform bonding thickness. Test specimens were compressed with Hoffman clamps and put into a preheated convection oven to cure the resins for 2 h at 120 °C; the samples were then subjected to a postcuring step for 2 h at 165 °C. The final specimen geometry is shown in [Figure S17](#). The lap shear strength was calculated by [eq 5](#). At least three parallel specimens were tested for each epoxy resin, and the average results were reported ([Figures S15](#) and [S16](#)).

$$\begin{aligned} \text{lap shear strength (psi)} \\ = 145.038 \times \text{maximum loading force (N)}/\text{bonding area (m}^2\text{)} \end{aligned} \quad (5)$$

■ ASSOCIATED CONTENT

Supporting Information

The Supporting Information is available free of charge on the ACS Publications website at DOI: [10.1021/acs.macromol.6b01861](https://doi.org/10.1021/acs.macromol.6b01861).

¹H NMR of the hardeners, DSC, isothermal DSC, TGA, FT-IR, tan δ vs temperature curves, lap shear tests and photo of lap shear specimens before and after pulling apart, hydrolytic degradation of Tr8SA/TTE polymers, and ¹H NMR of degraded products ([PDF](#))

■ AUTHOR INFORMATION

Corresponding Author

*E-mail treineke@umn.edu (T.M.R.).

Notes

The authors declare no competing financial interest.

■ ACKNOWLEDGMENTS

This work was supported by the NSF under the Center for Sustainable Polymers, CHE-1413862. Part of this work was carried out in the College of Science and Engineering Characterization Facility, University of Minnesota, which has received capital equipment funding from the NSF through the UMN MRSEC program under Award DMR-1420013. The authors thank Jeff Ting for his help with proofing this paper.

■ REFERENCES

- Barua, S.; Dutta, G.; Karak, N. Glycerol based tough hyperbranched epoxy: Synthesis, statistical optimization and property evaluation. *Chem. Eng. Sci.* **2013**, *95*, 138–147.
- Mondy, L. A.; Rao, R. R.; Moffat, H.; Adolf, D.; Celina, M. Structural epoxy foams. In *Epoxy Polymers: New Materials and Innovations*; Wiley-VCH: Weinheim, 2010.
- Tschan, M. J. L.; Brûlé, E.; Haquette, P.; Thomas, C. M. Synthesis of biodegradable polymers from renewable resources. *Polym. Chem.* **2012**, *3*, 836–851.
- Wang, C.; Venditti, R. A. UV Cross-Linkable Lignin Thermoplastic Graft Copolymers. *ACS Sustainable Chem. Eng.* **2015**, *3*, 1839–1845.
- Duarah, R.; Karak, N. A starch based sustainable tough hyperbranched epoxy thermoset. *RSC Adv.* **2015**, *5*, 64456–64465.
- Wang, C.; Kelley, S. S.; Venditti, R. A. Lignin-based thermoplastic materials. *ChemSusChem* **2016**, *9*, 770–783.
- Okada, H.; Tokunaga, T.; Liu, X.; Takayanagi, S.; Matsushima, A.; Shimohigashi, Y. Direct evidence revealing structural elements essential for the high binding ability of bisphenol A to human estrogen-related receptor-γ. *Environ. Health Perspect.* **2008**, *116*, 32.
- Auvergne, R.; Caillol, S.; David, G.; Boutevin, B.; Pascault, J. P. Biobased thermosetting epoxy: present and future. *Chem. Rev.* **2014**, *114*, 1082–1115.
- vom Saal, F. S.; Hughes, C. An extensive new literature concerning low-dose effects of bisphenol A shows the need for a new risk assessment. *Environ. Health Perspect.* **2005**, *113*, 926.
- Mekonnen, T.; Musrone, P.; Khalil, H.; Bressler, D. Progress in bio-based plastics and plasticizing modifications. *J. Mater. Chem. A* **2013**, *1*, 13379–13398.
- Shin, H.; Olsen, B. D.; Khademhosseini, A. The mechanical properties and cytotoxicity of cell-laden double-network hydrogels based on photocrosslinkable gelatin and gellan gum biomacromolecules. *Biomaterials* **2012**, *33*, 3143–3152.
- Feng, X.; East, A. J.; Hammond, W.; Jaffe, M. Sugar-based chemicals for environmentally sustainable applications in *ACS Symp. Ser.* **2010**, *1061*, 3–27 10.1021/bk-2010-1061.ch001.
- Feng, X.; East, A. J.; Hammond, W. B.; Zhang, Y.; Jaffe, M. Overview of advances in sugar-based polymers. *Polym. Adv. Technol.* **2011**, *22*, 139–150.
- Hong, J.; Radočić, D.; Ionescu, M.; Petrović, Z. S.; Eastwood, E. Advanced materials from corn: isosorbide-based epoxy resins. *Polym. Chem.* **2014**, *5*, 5360–5368.
- Chrysanthos, M.; Galy, J.; Pascault, J.-P. Preparation and properties of bio-based epoxy networks derived from isosorbide diglycidyl ether. *Polymer* **2011**, *52*, 3611–3620.
- Lukaszczuk, J.; Janicki, B.; Kaczmarek, M. Synthesis and properties of isosorbide based epoxy resin. *Eur. Polym. J.* **2011**, *47*, 1601–1606.
- Deng, J.; Liu, X.; Li, C.; Jiang, Y.; Zhu, J. Synthesis and properties of a bio-based epoxy resin from 2,5-furandicarboxylic acid (FDCA). *RSC Adv.* **2015**, *5*, 15930–15939.
- Schiraldi, C.; Di Lernia, I.; De Rosa, M. Trehalose production: exploiting novel approaches. *Trends Biotechnol.* **2002**, *20*, 420–425.
- Yoshida, M.; Nakamura, N.; Horikoshi, K. Production of Trehalose from Starch by Maltose Phosphorylase and Trehalose Phosphorylase from a Strain of *Plesiomonas*. *Starch* **1997**, *49*, 21–26.
- Biwer, A.; Antranikian, G.; Heinzel, E. Enzymatic production of cyclodextrins. *Appl. Microbiol. Biotechnol.* **2002**, *59*, 609–617.
- Uekama, K.; Hirayama, F.; Irie, T. Cyclodextrin drug carrier systems. *Chem. Rev.* **1998**, *98*, 2045–2076.
- Sizovs, A.; Xue, L.; Tolstyka, Z.; Ingle, N. P.; Wu, Y.; Cortez, M.; Reineke, T. M. Poly(trehalose): sugar-coated nanocomplexes promote stabilization and effective polyplex-mediated siRNA delivery. *J. Am. Chem. Soc.* **2013**, *135*, 15417–15424.
- Teramoto, N.; Arai, Y.; Shibasaki, Y.; Shibata, M. A facile synthesis of a novel polyacetal containing trehalose residue in the main chain. *Carbohydr. Polym.* **2004**, *56*, 1–6.
- Kukowka, S.; Maslinska-Solich, J. S. α,α -Trehalose-based polyacetals and macrocyclic acetals. *Carbohydr. Polym.* **2010**, *80*, 711–719.
- Teramoto, N.; Unosawa, M.; Matsushima, S.; Shibata, M. Synthesis and properties of thermoplastic alternating copolymers

containing trehalose and siloxane units by hydrosilylation reaction. *Polym. J.* **2007**, *39*, 975–981.

(26) Teramoto, N.; Arai, Y.; Shibata, M. Thermoreversible Diels-Alder polymerization of difurfurylidene trehalose and bismaleimides. *Carbohydr. Polym.* **2006**, *64*, 78–84.

(27) Srinivasachari, S.; Liu, Y.; Prevette, L. E.; Reineke, T. M. Effect of trehalose click polymer length on pDNA complex stability and delivery efficacy. *Biomaterials* **2007**, *28*, 2885–2898.

(28) Srinivasachari, S.; Liu, Y.; Zhang, G.; Prevette, L.; Reineke, T. M. Trehalose click polymers inhibit nanoparticle aggregation and promote pDNA delivery in serum. *J. Am. Chem. Soc.* **2006**, *128*, 8176–8184.

(29) Anderson, K.; Sizovs, A.; Cortez, M.; Waldron, C.; Haddleton, D. M.; Reineke, T. M. Effects of trehalose polycation end-group functionalization on plasmid DNA uptake and transfection. *Biomacromolecules* **2012**, *13*, 2229–2239.

(30) Kizjakina, K.; Bryson, J. M.; Grandinetti, G.; Reineke, T. M. Cationic glycopolymers for the delivery of pDNA to human dermal fibroblasts and rat mesenchymal stem cells. *Biomaterials* **2012**, *33*, 1851–1862.

(31) Xue, L.; Ingle, N. P.; Reineke, T. M. Highlighting the role of polymer length, carbohydrate size, and nucleic acid type in potency of glycopolycation agents for pDNA and siRNA delivery. *Biomacromolecules* **2013**, *14*, 3903–3915.

(32) Cheng, J.; Khin, K. T.; Jensen, G. S.; Liu, A.; Davis, M. E. Synthesis of linear, beta-cyclodextrin-based polymers and their camptothecin conjugates. *Bioconjugate Chem.* **2003**, *14*, 1007–1017.

(33) Renard, E.; Volet, G.; Amiel, C. Synthesis of a novel linear water-soluble β -cyclodextrin polymer. *Polym. Int.* **2005**, *54*, 594–599.

(34) Reineke, T. M.; Davis, M. E. Structural effects of carbohydrate-containing polycations on gene delivery 1: carbohydrate size and its distance from charge centers. *Bioconjugate Chem.* **2003**, *14*, 247–254.

(35) Reineke, T. M.; Davis, M. E. Structural effects of carbohydrate-containing polycations on gene delivery 2: charge center type. *Bioconjugate Chem.* **2003**, *14*, 255–261.

(36) Srinivasachari, S.; Reineke, T. M. Versatile supramolecular pDNA vehicles via “click polymerization” of β -cyclodextrin with oligoethyleneamines. *Biomaterials* **2009**, *30*, 928–938.

(37) Nagashima, S.; Shimasaki, T.; Teramoto, N.; Shibata, M. Trehalose-incorporated polymer network by thiol-ene photopolymerization. *Polym. J.* **2014**, *46*, 728–735.

(38) Yano, S.; Teramoto, N.; Miyamoto, R.; Nakajima, E.; Hashimoto, K.; Shibata, M. Fibroblast cell proliferation on photo-cured trehalose cinnamoyl ester thin films. *J. Bioact. Compat. Polym.* **2015**, *30*, 87–98.

(39) O’Shea, T. M.; Webber, M. J.; Aimetti, A. A.; Langer, R. Covalent incorporation of trehalose within hydrogels for enhanced long-term functional stability and controlled release of biomacromolecules. *Adv. Healthcare Mater.* **2015**, *4*, 1802–1812.

(40) Lee, J.; Ko, J. H.; Lin, E.-W.; Wallace, P.; Ruch, F.; Maynard, H. D. Trehalose hydrogels for stabilization of enzymes to heat. *Polym. Chem.* **2015**, *6*, 3443–3448.

(41) Tang, S.; Kong, L.; Ou, J.; Liu, Y.; Li, X.; Zou, H. Application of cross-linked beta-cyclodextrin polymer for adsorption of aromatic amino acids. *J. Mol. Recognit.* **2006**, *19*, 39–48.

(42) Miyamae, K.; Nakahata, M.; Takashima, Y.; Harada, A. Self-healing, expansion–contraction, and shape-memory properties of a preorganized supramolecular hydrogel through host–guest interactions. *Angew. Chem., Int. Ed.* **2015**, *54*, 8984–8987.

(43) Alsbiae, A.; Smith, B. J.; Xiao, L.; Ling, Y.; Helbling, D. E.; Dichtel, W. R. Rapid removal of organic micropollutants from water by a porous β -cyclodextrin polymer. *Nature* **2015**, *529*, 190–194.

(44) Patel, M. K.; Davis, B. G. Flow chemistry kinetic studies reveal reaction conditions for ready access to unsymmetrical trehalose analogues. *Org. Biomol. Chem.* **2010**, *8*, 4232–4235.

(45) Deng, S.; Gangadharmath, U.; Chang, W. T. Sonochemistry: a powerful way of enhancing the efficiency of carbohydrate synthesis. *J. Org. Chem.* **2006**, *71*, 5179–5185.

(46) Park, S.-J.; Kim, T.-J.; Kim, H.-Y. Thermal and mechanical properties of diglycidylether of bisphenol A/ trimethylolpropane triglycidylether epoxy blends cured with benzylpyrazinium salts. *Polym. Int.* **2002**, *51*, 386–392.

(47) Liu, W. B.; Qiu, Q. H.; Wang, J.; Huo, Z. C.; Sun, H. Curing kinetics and properties of epoxy resin–fluorenyl diamine systems. *Polymer* **2008**, *49*, 4399–4405.

(48) Kissinger, H. E. Variation of peak temperature with heating rate in differential thermal analysis. *J. Res. Natl. Bur. Stand.* **1956**, *57*, 217–221.

(49) Ozawa, T. A modified method for kinetic analysis of thermoanalytical data. *J. Therm. Anal.* **1976**, *9*, 369–373.

(50) Ma, S.; Liu, X.; Fan, L.; Jiang, Y.; Cao, L.; Tang, Z.; Zhu, J. Synthesis and properties of a bio-based epoxy resin with high epoxy value and low viscosity. *ChemSusChem* **2014**, *7*, 555–562.

(51) Wan, J.; Gan, B.; Li, C.; Molina-Aldareguia, J.; Li, Z.; Wang, X.; Wang, D.-Y. A novel biobased epoxy resin with high mechanical stiffness and low flammability: synthesis, characterization and properties. *J. Mater. Chem. A* **2015**, *3*, 21907–21921.

(52) Patil, N. V.; Netravali, A. N. Nonedible starch based “green” thermoset resin obtained via esterification using a green catalyst. *ACS Sustainable Chem. Eng.* **2016**, *4*, 1756–1764.

(53) Kleiner, L. K. Stent formed from crosslinked bioabsorbable polymer. U.S. Patent 8,846,071 B2, Sept 30, 2014.

(54) Campbell, F. C. *Structural Composite Materials*; ASM international: Material Park, OH, 2010; pp 75–76.

(55) Hazer, B.; Hazer, D. B.; Coban, B. Synthesis of microbial elastomers based on soybean oil. Autoxidation kinetics, thermal and mechanical properties. *J. Polym. Res.* **2010**, *17*, 567–577.

(56) Tan, S. G.; Chow, W. S. Thermal properties, curing characterization and water adsorption of soybean oil-based thermoset. *eXPRESS Polym. Lett.* **2011**, *5*, 480–492.

(57) Rials, G.; Glasser, G. Engineering plastics from lignin - IV. Effect of crosslink density on polyurethane film properties – Variation in NCO:OH ratio. *Holzforschung* **1984**, *38*, 191–199.

(58) Lakes, R. S. High damping composite materials: Effect of structural hierarchy. *J. Compos. Mater.* **2002**, *36*, 287–297.

(59) Nielsen, L. E.; Landel, R. F. *Mechanical Properties of Polymers and Composites*, 2nd ed.; Marcel Dekker: New York, 1994.

(60) Semoto, T.; Tsuji, Y.; Yoshizawa, K. Molecular understanding of the adhesive force between a metal oxide surface and an epoxy resin. *J. Phys. Chem. C* **2011**, *115*, 11701–11708.

(61) Nakazawa, M. Mechanism of adhesion of epoxy resin to steel surface. *Nippon Steel Technical Report* **1964**, *63*, 16–22.

(62) Glazer, J. Monolayer studies of some ethoxylin resin adhesives and related compounds. *J. Polym. Sci.* **1954**, *13*, 355–369.

(63) Accurso, A. A.; Delaney, M.; O’Brien, J.; Kim, H.; Iovine, P. M.; Diaz, D. D.; Finn, M. G. Improved metal-adhesive polymers from copper(I)-catalyzed azide-alkyne cycloaddition. *Chem. - Eur. J.* **2014**, *20*, 10710–10719.

(64) Bender, M. L.; Ladenheim, H.; Chen, M. C. Acylium ion formation in the reactions of carboxylic acid derivatives. II. The hydrolysis and oxygen exchange of methyl mesitoate in sulfuric acid. *J. Am. Chem. Soc.* **1961**, *83*, 123–127.